The role of lubricants, scanning velocity and operating environment in adhesion, friction and wear of Pt–Ir coated probes for atomic force microscope probe-based ferroelectric recording technology

2008 J. Phys.: Condens. Matter 20 325240

(http://iopscience.iop.org/0953-8984/20/32/325240)

J. Phys.: Condens. Matter **20** (2008) 325240 (13pp) doi:10.1088/0953-8984/20/32/325240

The role of lubricants, scanning velocity and operating environment in adhesion, friction and wear of Pt–Ir coated probes for atomic force microscope probe-based ferroelectric recording technology

Bharat Bhushan[1] **and Kwang Joo Kwak**

Nanotribology Laboratory for Information Storage and MEMS/NEMS,
The Ohio State University, 201 West 19th Avenue, Columbus, OH 43210, USA

E-mail: bhushan.2@osu.edu

Received 5 June 2008, in final form 1 July 2008
Published 21 July 2008
Online at stacks.iop.org/JPhysCM/20/325240

Abstract

Probe-based data recording is being developed as an alternative technology for ultrahigh areal density. In potential ferroelectric data storage, a conductive atomic force microscope tip is scanned over a lead zirconate titanate (PZT) film, a ferroelectric material. The understanding and the improvement of wear of the tip during its contact with the ferroelectric materials is critical, particularly at the high scanning velocities needed for high data rate recording in the operating environments. To this end, adhesion, friction and wear experiments are performed using Pt–Ir coated tips sliding against unlubricated and lubricated PZT films at velocities ranging from 0.1 to 100 mm s^{-1}, the maximum velocity corresponding to the expected recording rate. Two lubricants were used: perfluoropolyether and ionic liquid. The Pt–Ir tips are shown to exhibit lower wear against the lubricated PZT film. To study the role of the operating environment, experiments are also conducted at 80 and 120 °C and at 5–80% relative humidity. Relevant wear mechanisms are discussed.

1. Introduction

With the advent of scanning probe microscopes (SPM), probe-based data recording techniques are being developed for ultrahigh areal density. Many approaches using thermomechanical, phase change, magnetic, thermomagnetic, optical, electrical and ferroelectric methods have been demonstrated (Bhushan 2007, Kwak and Bhushan 2008). One of the new alternative ferroelectric data storage methods is a mechanically-addressed recording system using a probe-based storage device with atomic force microscope (AFM) tips. A schematic for domain writing and reading in ferroelectric films is shown in figure 1. A conductive AFM tip is placed in contact with a $PbZr_{0.52}Ti_{0.48}O_3/SrRuO_3$ (PZT/SRO) double layer (Franke *et al* 1994, Hidaka *et al* 1996, Ahn *et al* 1997, Shin *et al* 2002). The SRO serves as the bottom electrode, and PZT represents the ferroelectric film. Ferroelectric domains can be polarized by applying short voltage pulses (∼10 V, ∼100 μs) between the AFM tip and the SRO electrode that exceed the coercive field of the PZT layer, resulting in local, nonvolatile changes in the electronic properties of the underlying film. The PZT surface is in contact with the probe tip during writing, and the scanning is performed at high velocities for high data rate recording.

Crucial mechanical reliability concerns in probe-based data storage are stiction, friction and wear of the tip after repeated tip–surface contact at high scanning velocities in the operating environment after prolonged device operation (Bhushan 2002, 2005). PZT has a high hardness and an elastic modulus of about 13 and 200 GPa, respectively (Palacio and Bhushan 2008a). Pt-based tips such as Pt–Ir commonly considered for this application have relatively low hardness.

[1] Author to whom any correspondence should be addressed.

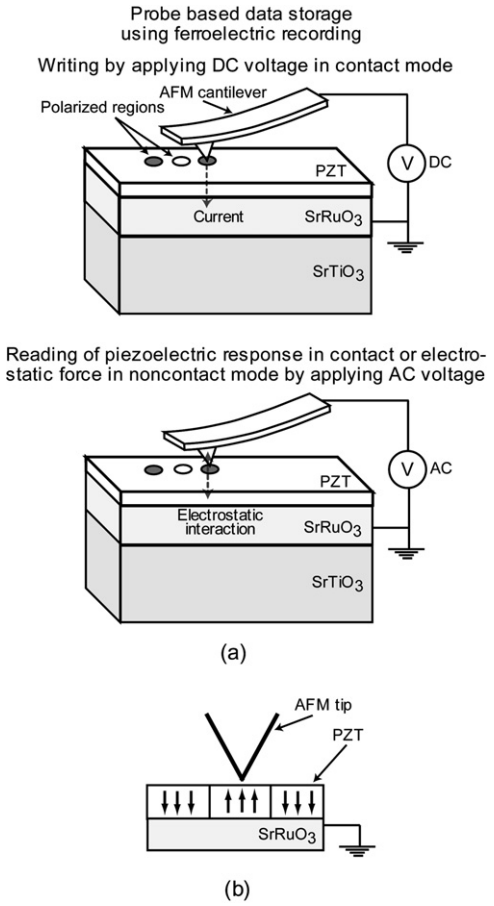

Figure 1. Schematics of the AFM probe-based storage system using ferroelectric media.

The reported values for hardness of Pt and Ir are 0.36 and 2.2 GPa and for elastic modulus are 171 and 517 GPa, respectively (Davis 1998). However, the composite hardness and elastic modulus at a given penetration depth are also dependent upon the base Si tip and are reported to be high (Palacio and Bhushan 2008b). A sharp coated Si tip with 50 nm radius in contact with a PZT surface at a normal load of 100 nN is expected locally to go through plastic deformation. The local stresses would then be comparable to the surface hardness which makes the tip and the sample susceptible to deformation. Possible wear mechanisms of AFM tip–sample contacts include adhesive wear, abrasive wear, low cycle fatigue, impact wear, tribochemical wear, and thermally-activated stick-slip (Bhushan and Kwak 2007a, 2007b, 2008a, 2008b, Kwak and Bhushan 2008, Palacio and Bhushan 2008b). The tribological properties are strongly dependent on the sliding velocity and the operating environment including temperature and relative humidity. The sliding velocity has an especially important role on nanoscale wear resistance for high data rate recording.

In order to improve tribological performance, lubricants need to be applied to the surface of interest. The ideal lubricant should be molecularly thick, easily applied, able to chemically bond to the micro/nanodevice surface, insensitive to the environment, and highly durable (Bhushan 1996, Liu and Bhushan 2003, Tao and Bhushan 2005a, 2005b). Liquid lubricants that can be chemically bonded to the PZT film are attractive candidates for tip and medium coating. Chemically bonded liquid lubricants of perfluoropolyethers (PFPEs) are widely used in the construction of magnetic rigid disks and metal evaporated tapes (Bhushan 1996). Ionic liquids are considered as potential lubricants as well (Bhushan *et al* 2008, Palacio and Bhushan 2008a, 2008c). Unlike conventional lubricants that are electrically insulating, ionic liquids can minimize the contact resistance between sliding surfaces because they are conducting, and conducting lubricants are needed for various electrical applications. These liquids can also be used to mitigate arcing, which is a cause of electrical breakdown in sliding electrical contacts (Campbell 1978). In addition, ionic liquids have high thermal conductivity which helps to dissipate heat during sliding (Van Valkenburg *et al* 2002). An ionic liquid is a synthetic salt with a melting point below 100 °C. In ionic liquid, one or both of the ions are an organic species. At least one ion has a delocalized charge such that the formation of a stable-crystal lattice is prevented and the ions are held together by strong electrostatic forces.

In this work, two coatings including a PFPE lubricant, Z-TETRAOL, and an ionic lubricant, BMIM-PF_6, are applied on PZT films in order to reduce the adhesion, friction and wear of a probe tip. A comprehensive investigation of adhesion, friction and wear of a Pt–Ir coated tip sliding against unlubricated and lubricated PZT films is performed at two loads as a function of sliding distance, velocity, temperature and humidity. The adhesive force, coefficient of friction and wear are measured and tip wear mechanisms are discussed.

2. Experimental details

2.1. Experimental samples

The probes used in this study were etched single-crystal silicon probes coated with Pt–Ir films. The rectangular silicon cantilevers with pyramidal probe tips (PPP-EFM, Nanosensors) were coated with 25 nm/3 nm thick Pt–Ir/Cr (figure 2). The nominal spring constant of the cantilever was 2.8 N m^{-1}, and the tip radius was 10 nm before coating and 53 nm after coating with Pt–Ir and Cr (provided by the manufacturer; Bhushan and Kwak 2008a).

A PZT film was deposited on a 50 nm thick $SrRuO_3$ (SRO) film grown by pulse laser deposition (PLD) on 0.5 mm thick *c*-axis $SrTiO_3$ (STO) substrate. PLD was also used to deposit the 50 nm thick PZT film with a Zr/Ti composition ratio of 20/80 ($PbZr_{0.2}Ti_{0.8}O_3$). The surface morphology was observed using an AFM with a 10×10 μm^2 scan, and the RMS roughness of the PZT film was about 2 nm.

The lubricants used in this study are the perfluoropolyether (PFPE) lubricant Z-TETRAOL 2000 (Solvay Solexis Inc.) and the ionic liquid 1-butyl-3-methylimidazolium hexafluorophosphate, abbreviated as BMIM-PF_6 (Merck). Z-TETRAOL 2000, referred to as Z-TETRAOL, is a derivate of PFPEs with a double hydroxyl (–OH) group at each end of the polymer chain. Their chemical formulas are shown in figure 3(a). The two liquids have comparable decomposition temperatures, but the

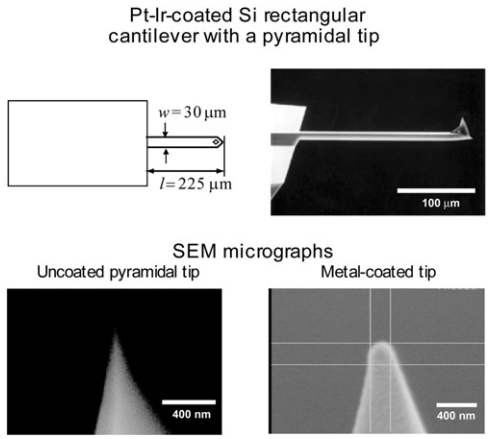

Figure 2. Schematics and photographs of rectangular cantilever with single-crystal silicon probes coated with Pt–Ir film.

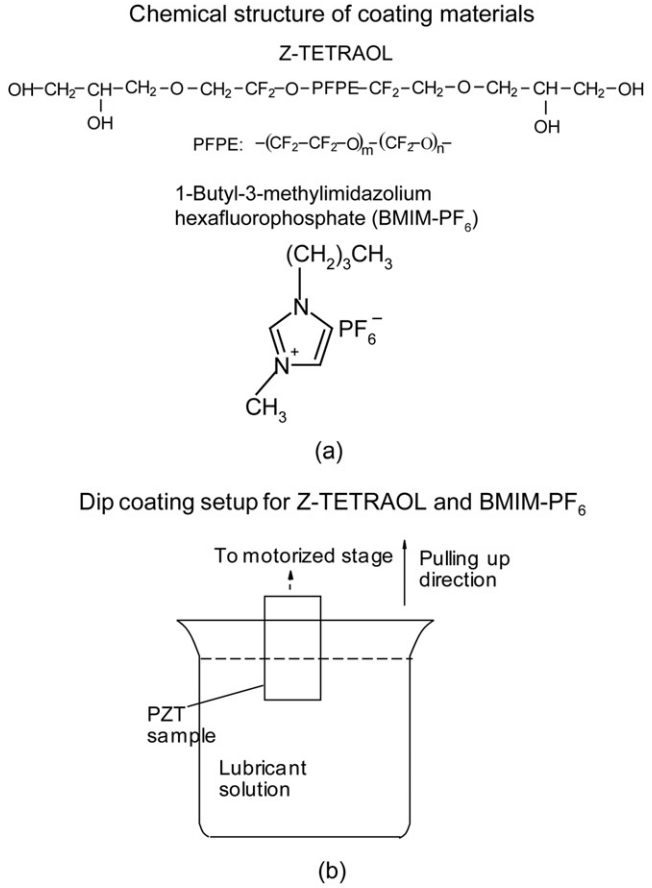

Figure 3. (a) Chemical structures of Z-TETRAOL and BMIM-PF_6, and (b) a schematic of dip coating technique for Z-TETRAOL and BMIM-PF_6.

ionic liquid has a higher specific heat capacity and thermal conductivity (Bhushan *et al* 2008, Palacio and Bhushan 2008a). Both liquids have very low vapor pressure, which makes them ideal lubricants.

The two liquids were applied on PZT using the dip coating technique, figure 3(b). The method and the apparatus used have been described elsewhere (Liu and Bhushan 2003, Tao and Bhushan 2005a). Briefly, the test samples were ultrasonicated in acetone followed by isopropanol and deionized water for 5 min each. Then, the test sample was vertically submerged into a beaker containing a dilute solution of the lubricant for 10 min. The solutions of the various lubricants are 0.025% (v/v) Z-TETRAOL in HFE 7100 (a solvent consisting of isomers of methoxynonafluorobutane ($C_4F_9OCH_3$)) and 0.1% (v/v) BMIM-PF_6 in isopropanol. Both solutions were mixed vigorously and allowed to stand for at least 1 h prior to use. The dip coating procedure is as follows. The PZT samples were pulled up from solution with the aid of the motorized stage set at constant speed of 5 mm s^{-1} to obtain films of desired thickness. Thermally treated samples were prepared by heating at 150 °C for 1 h after dip coating. The thermal treatment procedure facilitates the immobilization of lubricant, consisting of mobile and immobile fractions (Bhushan *et al* 2008, Palacio and Bhushan 2008a, 2008c). The samples were then measured with an ellipsometer in the fixed refractive index option (NFXD option, Gaertner Scientific L115C Ellipsometer Instruction Manual). The coating thickness was found to be about 2 and 3 nm for Z-TETRAOL and BMIM-PF_6, respectively.

2.2. Tip shape characterization

A silicon TGT1 grating sample (NT-MDT, Moscow, Russia) was used for probe tip characterization (Bhushan and Kwak 2007a, 2007b). The grating sample has an array of sharp tips on the surface (see figure 4(a)). The tips are arranged on each corner and at the center of a 3×3 μm^2 square area. The height of each tip is 0.4 μm. The tip angle is about 30°, and the radius of the tip is less than 10 nm. SPIP^{TM} software (Scanning Probe Image Processor, Image Metrology A/S, Denmark) was used to characterize the tip and evaluate the tip radius. The processing procedure is illustrated in figure 4(b). The image was first obtained in tapping mode by scanning the tip on the TGT1 grating sample in a direction perpendicular to the long axis of the cantilever beam. Scanning was performed on a 2×2 μm^2 scan area with a velocity of 1 μm s^{-1}. The 3D surface of the tip was generated with 970 nm × 970 nm size (63 points × 63 points) using a blind tip reconstruction algorithm from the scanned image (Villarrubia 1994). Even if the probe tip has an asymmetric shape, a simple semicircle could be more easily fitted on the 2D tip profile than a hemisphere to a 3D surface; therefore, a 2D tip radius was calculated. The algorithm was used to generate a 2D profile from the tip surface in the scanning direction at the highest location. Tip radius was calculated for a profile with several tens of nm in length by a circle fit with at least 5 data points (15.4 nm apart) using the SPIP software.

2.3. Adhesion, friction and wear measurements

Adhesion, friction and wear tests were conducted using a Dimension 3000 AFM (Digital Instruments). The adhesive forces were measured in ambient environment (22 ± 1 °C, 50 ± 5% relative humidity (RH)). The force calibration technique is used for adhesive force measurement. In this technique, the tip

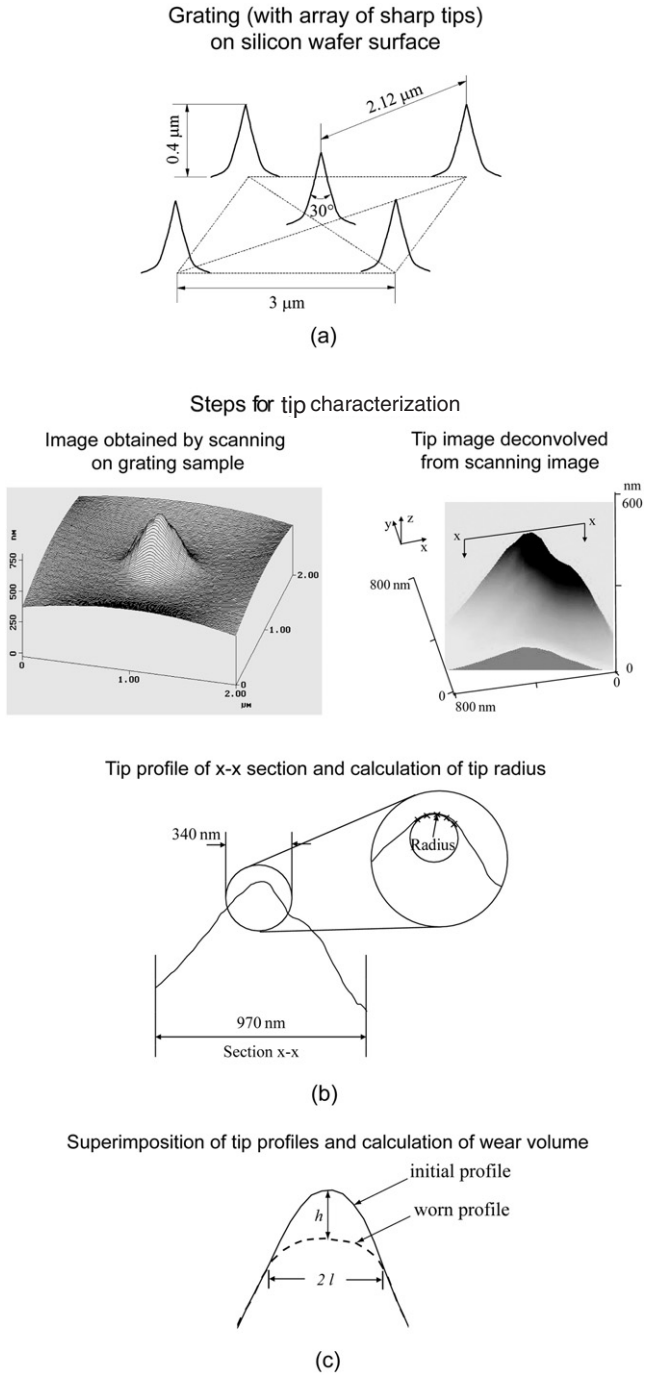

Figure 4. (a) A schematic of grating (with array of sharp tips) on silicon wafer surface, (b) illustration of tip characterization and calculation of tip radius, and (c) illustration of calculation of the wear volume.

is brought into contact with the sample and then pulled away at a frequency of 1 Hz. The force, needed to pull the apart from the sample, is measured as adhesive force (Bhushan 2002, 2005). Based on a minimum of three measurements, standard deviation of the data was ±10%.

The friction force experiments were carried out by scanning the sample along an axis perpendicular to the long axis of the cantilever at a scan velocity of 1 μm s^{-1} using a scan rate of 0.5 Hz at normal loads ranging from 1 to 120 nN. The effect of z-piezo movement on the normal load due to thermal drift was monitored and was found to be within 10%. The measured friction force was plotted as a function of normal load. The coefficient of friction was obtained by calculating the slope of the line (Ruan and Bhushan 1994, Bhushan 2002, 2005).

For wear experiments, a high velocity piezo stage, developed by Tao and Bhushan (2006a), was used at 10 mm s^{-1} (frequency = 10 Hz) and 100 mm s^{-1} (frequency = 50 Hz) sliding velocities. The system includes a custom calibrated piezo stage or a piezo ultrasonic linear drive (M663.465, Physik Instrumente, GmbH & Co. KG, Karlsruhe, Germany), a stage controller (C865, Physik Instrumente), and a self-designed software application for operation control. A sliding velocity of 10 mm s^{-1} was used for a maximum sliding distance of 100 m. A higher velocity at 100 mm s^{-1} was used for a total sliding distance of 300 m to reduce the test duration. The length of a single line scan for line profile mode was 500 and 1000 μm for average sliding velocities of 10 and 100 mm s^{-1}, respectively. For sliding distances of 1, 3, 10, 30 and 100 m, sliding duration was 1×10^2, 3×10^2, 1×10^3, 3×10^3 and 1×10^4 s at sliding velocities of 10 mm s^{-1}, respectively. For the remaining 200 m distance, sliding duration was 2×10^3 s at sliding velocities of 100 mm s^{-1}. Scan direction was parallel to the long axis of cantilever beam.

For wear measurements, each probe was first scanned on the grating sample in tapping mode to obtain the initial image for tip characterization (Bhushan and Kwak 2007a). After scanning on the grating sample, the tip was slid on a PZT film sample in contact mode. After the wear test, the probe was scanned again on the grating sample to obtain an image for tip characterization. The wear volume was calculated from the tip profiles before and after the wear experiment. In order to calculate the wear volume, the profile after sliding was manually superimposed with the original profile so that they coincide (largely) with each other, see figure 4(c). The worn region was assumed to be cone-shaped. The worn height (h) of the cone was the distance between the tops of the original and worn tips, and the $2l$ was the width of the base of the worn region. The wear volume was calculated as $V = \pi l^2 h/3$.

To further understand the wear mechanisms, the worn tips were imaged using a field emission scanning electron microscope (FE-SEM; Hitachi S-4300) operating at 10 kV and 5 μA under 1.2×10^{-7} Pa. The virgin tips were examined for reference as well as to check the uniformity of the top metal coating.

In addition, experiments were conducted to study the effect of velocity, temperature and relative humidity on the unlubricated PZT as well as lubricated with a lubricant with lower adhesion, friction, and wear properties. Experimental details follow.

2.3.1. Effect of velocity at two loads. The wear experiments were performed at sliding velocities ranging from 0.1 to 100 mm s^{-1} by applying a normal load of 50 nN followed by 100 nN in the line profile mode. All experiments at various

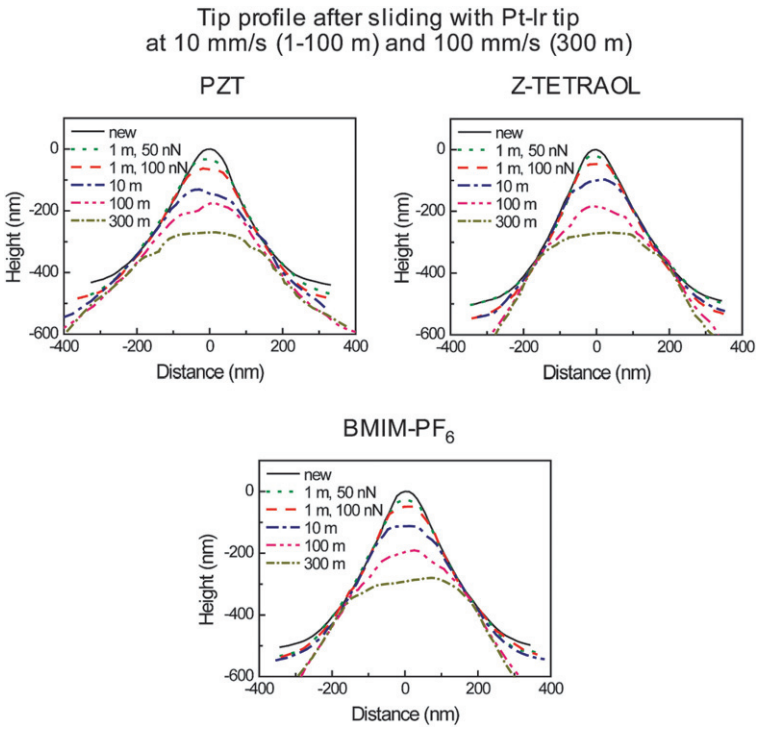

Figure 5. Pt–Ir tip profiles before and after 1 m sliding, 10 mm s^{-1} and at 50 nN followed by 1 m sliding at 100 nN, and after 10 and 100 m sliding at 10 mm s^{-1} and at 100 nN, and 300 m sliding at 100 mm s^{-1} and at 100 nN on unlubricated and lubricated PZT films. The solid curve corresponds to the virgin tip profiles.

velocities were performed for a constant sliding distance of 1 m at given loads in order to have the same sliding distance for the tip. The length of a single line scan in the line profile mode was 25, 50, 100, 500 and 1000 μm for average sliding velocities of 0.1, 0.25, 1, 10 and 100 mm s^{-1}, respectively. At 0.1 and 0.25 mm s^{-1} sliding velocities, standard AFM scanner was used. For experiments from 1 to 100 mm s^{-1}, the high velocity piezo stage was used. However, the number of cycles (round trips), which are relevant, are not same at different velocities. For velocities of 0.1, 0.25, 1, 10 and 100 mm s^{-1}, number of cycles are 2×10^4, 1×10^4, 5×10^3, 1×10^3 and 5×10^2, respectively. This means that PZT samples see decreasing number of cycles with an increase in velocity; consequently, it has an effect on wear rates and worn images at different velocities.

2.3.2. Effect of temperature at two loads. The effect of temperature experiments were conducted using a home-made thermal stage capable of temperatures up to 125 °C (Liu and Bhushan 2003). The heat-generating elements were Ohmic resistors encapsulated in a steel holder and kept in good thermal contact by using thermal paste. A thermal controller and a solid-state relay were used to control the temperature by adjusting on/off time. The temperatures used were 22, 80 and 120 °C. During the experiments, the relative humidity (RH) of the chamber was maintained at 50 ± 10% RH. The sample and tip were kept in the environmental chamber for at least 1 h to allow the system to reach equilibrium. Experiments were performed at 0.1 mm s^{-1} and 50 nN for 1 m followed by at 100 nN for 1 m on 25 μm length.

2.3.3. Effect of relative humidity at two loads. The effect of relative humidity experiments were performed in the environmentally controlled chamber, in which the humidity was controlled by introducing a combination of dry N_2 and moist air. The relative humidity used was 5, 50 and 80% while the temperature was maintained at 22 ± 2 °C. During the experiments, the sample and tip were kept in the environment chamber for at least 1 h to allow the system to reach equilibrium. Experiments were performed at 0.1 mm s^{-1} and 50 nN for 1 m followed by at 100 nN for 1 m on 25 μm length.

3. Results and discussion

3.1. Adhesion, friction and wear of unlubricated and lubricated samples

Wear experiments were conducted with the unlubricated and lubricated PZT films at 50 and 100 nN in order to compare the wear resistance of the Pt–Ir tip. Figure 5 shows the tip profiles taken after sliding for 1, 10, 100 and 300 m. Reduction in height indicates tip blunting resulting from wear, and is seen in all cases. These profiles were compared with one taken before the wear experiment in order to calculate the wear volume; data is presented in figure 8 (to be discussed later). After sliding for 300 m, the Pt–Ir tip profile against Z-TETRAOL lubricated film showed less wear compared to that against the unlubricated PZT film. Ionic liquid also provides wear protection but less than that of Z-TETRAOL. Tip profiles provide evidence of an irregular worn surface, indicating abrasive wear, especially after long sliding distances. Brittle

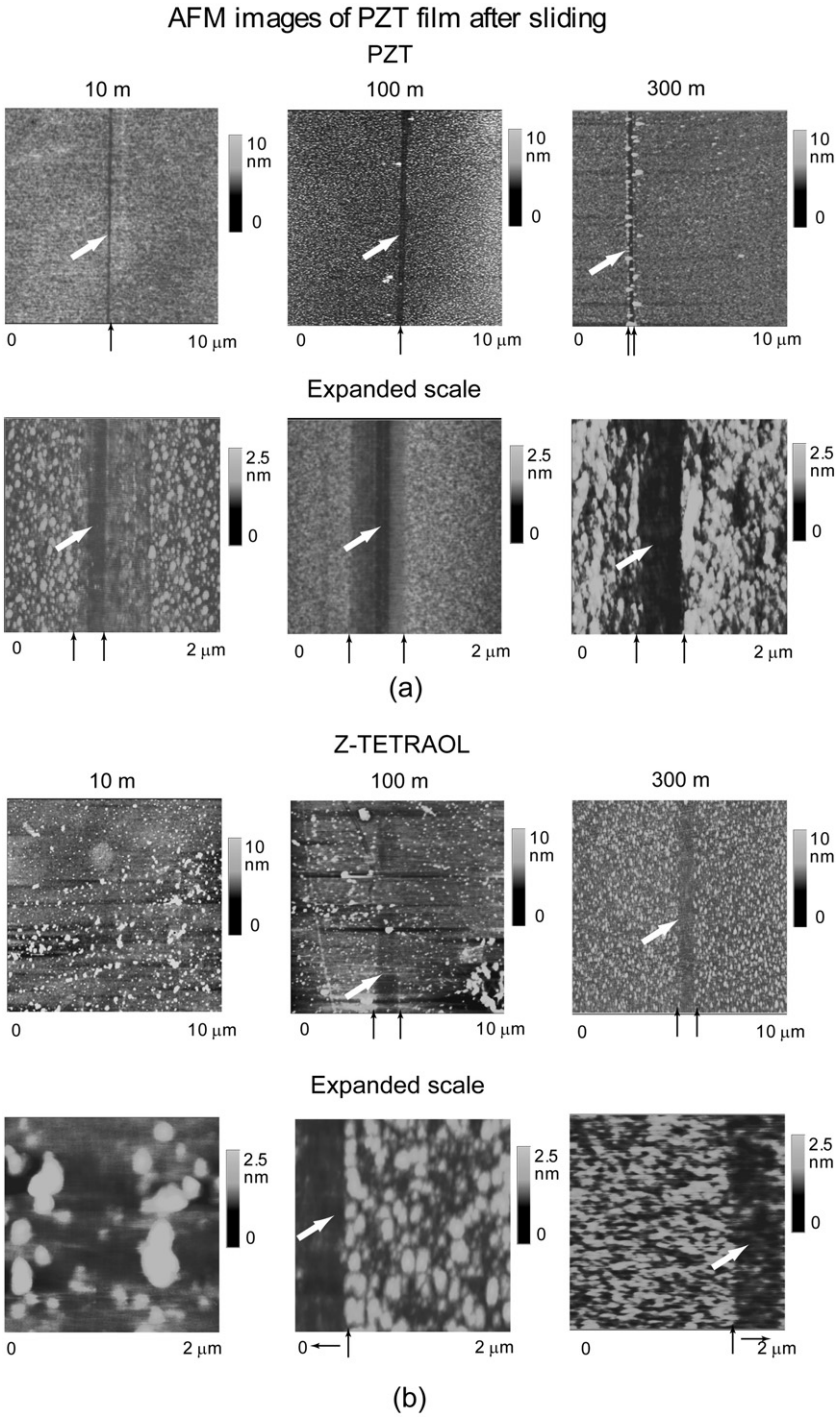

Figure 6. AFM images obtained after 10 and 100 m sliding with Pt–Ir tip at 10 mm s^{-1} and 100 nN, an additional 300 m sliding at 100 mm s^{-1} and 100 nN (a) on the unlubricated PZT film, and (b) on the Z-TETRAOL lubricated PZT film. Expanded scale images are shown in the bottom row. If wear scar can be detected, black arrows are used to identify them and white arrows indicate significant damage.

Pt–Ir-coated silicon asperities can fracture when sliding against the film surface. Particles would be produced by the fracture of asperities. These particles stay between the contacting surfaces and could accelerate the abrasive wear (Bhushan 2002, 2005, Tao and Bhushan 2006b).

Figure 6(a) shows AFM surface height images obtained after sliding for 10, 100 and 300 m at 100 nN on the PZT film. The PZT surface worn by the Pt–Ir tip shows visible wear scars. If a wear scar can be detected, black arrows are used to identify them, and white arrows indicate significant damage. In some cases, e.g., after 100 m sliding, band-type wear scars in expanded images are observed due to blunting of the tip as well as the thermal drift after sliding for 167 min (to attain 100 m sliding distance). The wear depth of PZT against Pt–Ir tip is observed to be about 1 nm. AFM images of wear scars show plowing of PZT material and pile up in the wear tracks,

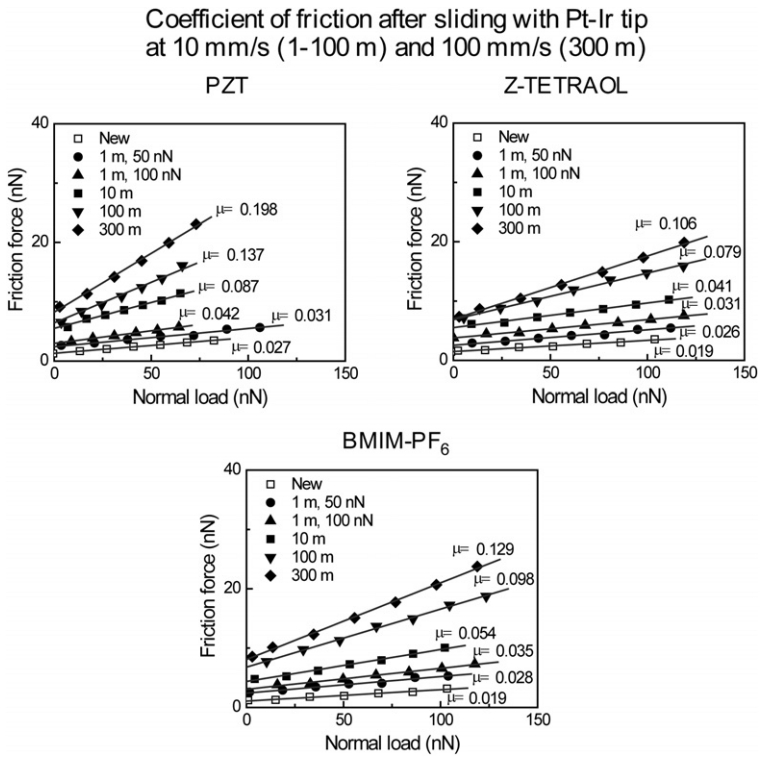

Figure 7. Friction force as a function of normal load, obtained by measuring friction forces with Pt–Ir tips at increasing normal loads in range of 1–120 nN after 1, 10, 100 and 300 m sliding on the PZT films. The coefficient of friction can be obtained by calculating the slope of the line.

which is indicative of adhesive wear. However, a wear scar was not observed after 1 m of sliding at 100 nN on the PZT film. The sliding cycles (round trips) were only 1000 cycles during 1 m sliding. Figure 6(b) shows AFM surface height images obtained after sliding for 10, 100 and 300 m at 100 nN on the Z-TETRAOL lubricated film. The lubricated surface worn by the Pt–Ir tip also shows visible wear scars. The wear depth of the lubricated film against Pt–Ir tip is observed to be about 0.5 nm.

The data for wear volumes and tip radii are summarized in figure 8 (to be presented later). The magnitude of the wear volume and its rate of increase against Z-TETRAOL lubricated film are lower than that against the unlubricated PZT film. The BMIM-PF_6 lubricated film also provides wear protection but less than that of Z-TETRAOL. In all cases, the increase in wear volume is more significant at larger sliding distance, and the progressive damage is responsible for an increase in the wear rate. For example, the wear volume against the unlubricated film and the Z-TETRAOL lubricated film after sliding for a distance of 100 m are 3.4×10^6 and 2.8×10^6 nm^3, however, after sliding of 300 m are 6.6×10^6 and 4.2×10^6 nm^3, respectively.

In order to investigate the friction properties between the tips and the PZT films, the friction force as a function of normal load was measured. Figure 7 presents the friction force as a function of normal load before sliding and after sliding for 1, 10, 100 and 300 m. The values of friction force against unlubricated film are higher than those obtained against the lubricated films. The data could be fitted with a straight line, which suggests that friction force is proportional to normal load. Figure 8 also summarizes the coefficient of friction (μ) as a function of sliding distance. The coefficient of friction increases with an increase in the sliding distance. The rate of increase is higher at larger sliding distances, consistent with the trends in wear volume. For example, the coefficient of friction against the unlubricated film and the Z-TETRAOL lubricated film after sliding for a distance of 100 m are 0.14 and 0.08, however, after sliding of 300 m are 0.2 and 0.11, respectively.

Figure 8 also summarizes the adhesive force as a function of sliding distance. The value of the adhesive force at given sliding distance against Z-TETRAOL lubricated film is consistently lower than that against the unlubricated PZT film. The BMIM-PF_6 lubricated film presents comparable value but higher than that of Z-TETRAOL. The increase in the tip radius after sliding leads to a larger contact area leading to higher adhesion, which increases the friction force and the measured value of μ. For example, the adhesive force for unlubricated film and the Z-TETRAOL lubricated film after sliding for a distance for 100 m are 99 and 48 nN, and the tip radius after sliding for 100 m are 155 and 137 nm, respectively. It is noted that the rate of increase is higher at larger sliding distances, which is consistent with the trends in wear volume and coefficient of friction.

In addition to characterizing the probe tip using SPIP software, the tip shapes before and after sliding were imaged by a scanning electron microscope (SEM). Figure 9 shows SEM images of Pt–Ir tips before the wear experiments and after sliding for 300 m at a load of 100 nN. Blunting of the Pt–Ir tip against Z-TETRAOL lubricated film occurred to a lesser extent against the unlubricated film. Particularly, the

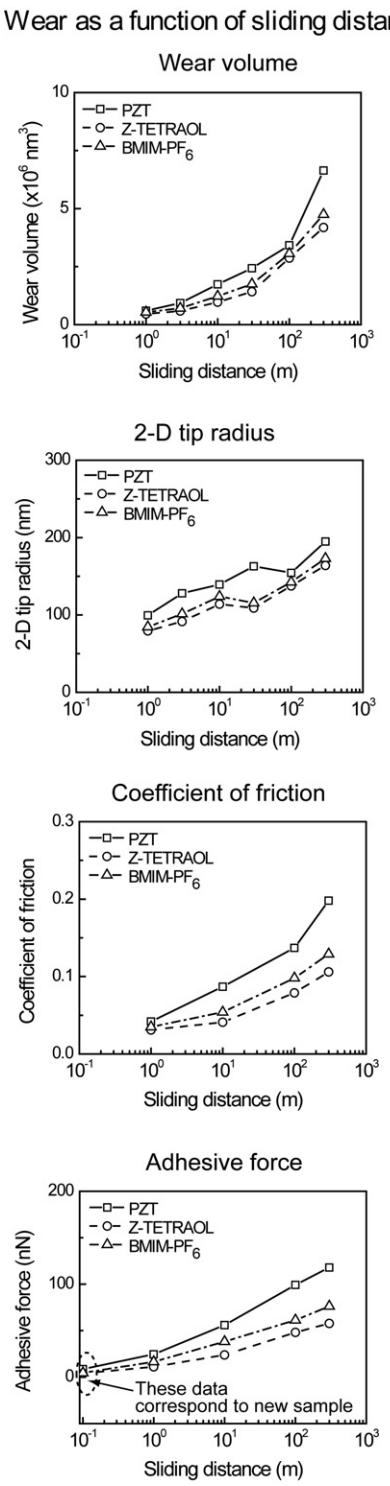

Figure 8. Wear volumes, 2D tip radii, coefficient of friction, and adhesive force as a function of sliding distance.

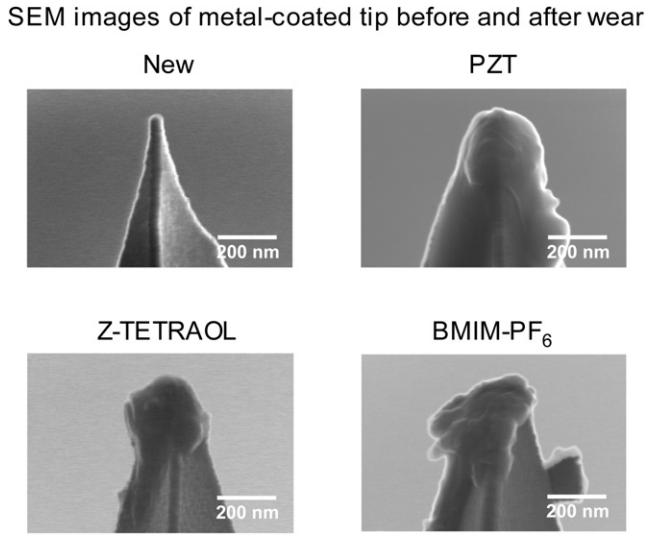

Figure 9. SEM images obtained before and after 300 m sliding at 100 nN on the unlubricated, Z-TETRAOL and BMIM-PF_6 lubricated PZT films.

exposed under-layer of the Si part is clearly observed in the tip against the unlubricated film. The post-wear experiment images corroborate the 2D tip profiles in figure 5. The tip is plastically deformed during wear; therefore, it can be deduced that the mechanism for tip wear is adhesive.

In summary, from SEM imaging and tip profiling, as well as AFM imaging of the PZT films, it was found that the Pt–Ir tips exhibit adhesive and abrasive wear. The wear, friction and adhesive forces increase with sliding distance, and the rate of increase is higher at larger sliding distances. Z-TETRAOL lubricated film exhibited the best performance and was selected for velocity, temperature and relative humidity studies.

3.2. Effect of velocity

The wear experiments were conducted using an AFM at a velocity range of 0.1–100 mm s^{-1}, and the data are presented in figure 10. The Z-TETRAOL lubricated film exhibits lower wear volumes than that of the unlubricated film. In the velocity range used, wear volumes ranged from 0.04×10^6 to 0.41×10^6 nm^3 after sliding at 50 nN and from 0.11×10^6 to 0.92×10^6 nm^3 after sliding at 100 nN. These are lower than the wear volumes of the unlubricated sample, which ranged from 0.07×10^6 to 0.61×10^6 nm^3 after sliding at 50 nN and from 0.19×10^6 to 1.3×10^6 nm^3 after sliding at 100 nN, in the velocity range used. The data presented clearly show that the use of Z-TETRAOL decreases tip wear. The tip radii and corresponding wear volume data for the unlubricated and lubricated films follow a similar trend.

Based on the Archard wear equation, the wear rate is proportional to the load and is independent of sliding distance and velocity (Bhushan 2002). Practical wear situation includes adhesive and abrasive wear, where the wear rate is dependent upon the sliding velocity. We observe in figure 10 that wear volume initially increases as a logarithm of sliding velocity at two loads, and then it increases with sliding velocity at a slower rate with a velocity exponent in a range of 0.06–0.11. We also observe that the coefficient of friction initially increases as a logarithm of sliding velocity at two loads, and then it increases with sliding velocity at a slower rate with a velocity exponent in the range of 0.017–0.021. The initial logarithm dependence for both friction and wear is based on the thermally-activated stick-slip mechanism (Tambe and Bhushan 2005, Tao and Bhushan 2007, Bhushan and Kwak 2007a, 2007b).

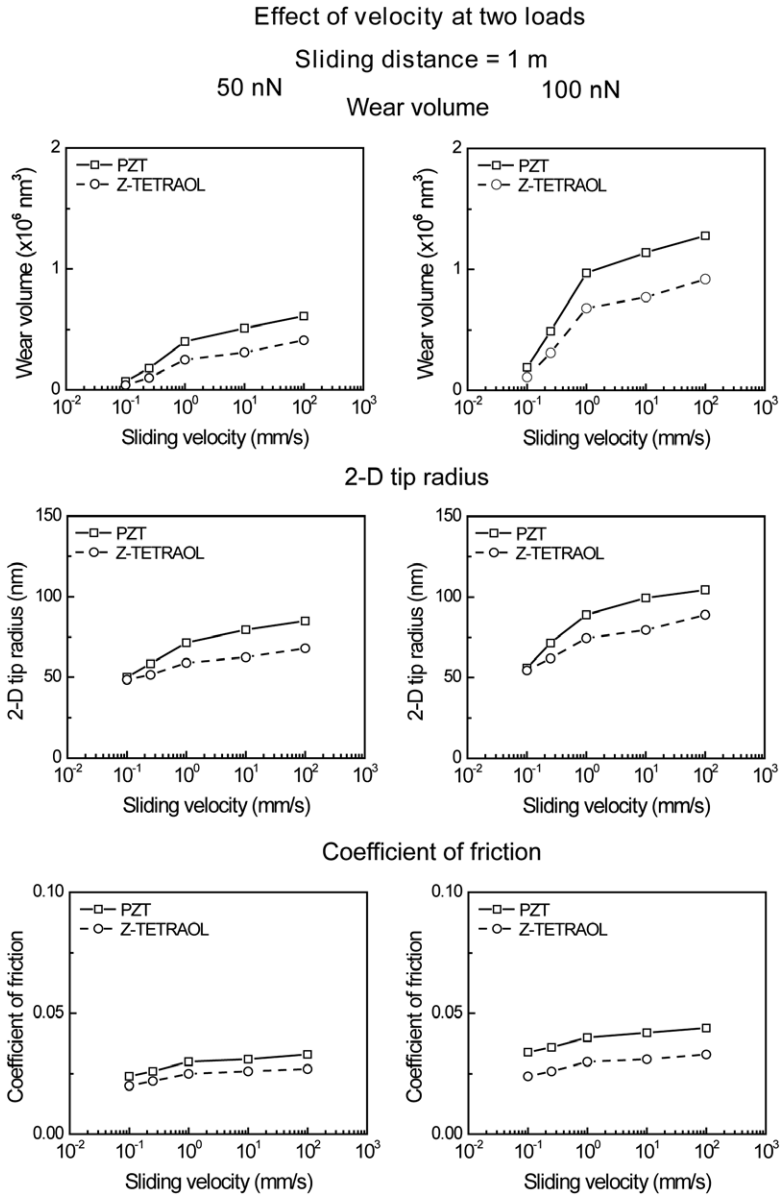

Figure 10. Wear volumes, 2D tip radii and coefficients of friction as a function of sliding velocity at two loads on the unlubricated and Z-TETRAOL lubricated PZT films.

At higher velocities, impact of asperities becomes important, and wear could be caused by the adhesive wear and periodical high velocity impact on the PZT film surface (Tambe and Bhushan 2005, Tao and Bhushan 2007, Bhushan and Kwak 2007a, 2007b, Kwak and Bhushan 2008).

As the energetic input into the tribological system is dissipated during the sliding process, the cumulative dissipated energy is equivalent to the work done on the system (Bhushan 2002, 2005). Therefore, the volume of wear is directly related to the energy dissipated by friction. This observation demonstrates the existence of a relationship between the mechanisms responsible for wear and friction.

3.3. Effect of temperature

Temperature plays a crucial role in wear, so high temperature experiments were conducted with the sample heated to 80 and 120 °C (Bhushan and Kwak 2008b). Figure 11 shows the wear volume, tip radius and coefficient of friction data after 1 m sliding at 50 nN, after additional 1 m sliding at 100 nN and 0.1 mm s^{-1} for the sample temperatures at 22, 80 and 120 °C. The temperature of the tip is expected to be lower than the temperature on the sample. Bhushan and Kwak (2008b) have reported the temperature difference to be on the order of 6 °C when the sample is heated to 80 °C. Based on the high temperature data in figure 11, wear rate increases with an increase in the sample temperature. The tip sliding on the unlubricated film exhibited a larger volume of wear at a given operating condition than that on Z-TETRAOL lubricated film surfaces.

It should be noted that the thickness of surface water layer is expected to decrease at higher temperature, which is responsible for meniscus forces. However, this source does not appear to be important for changes in friction and wear as a

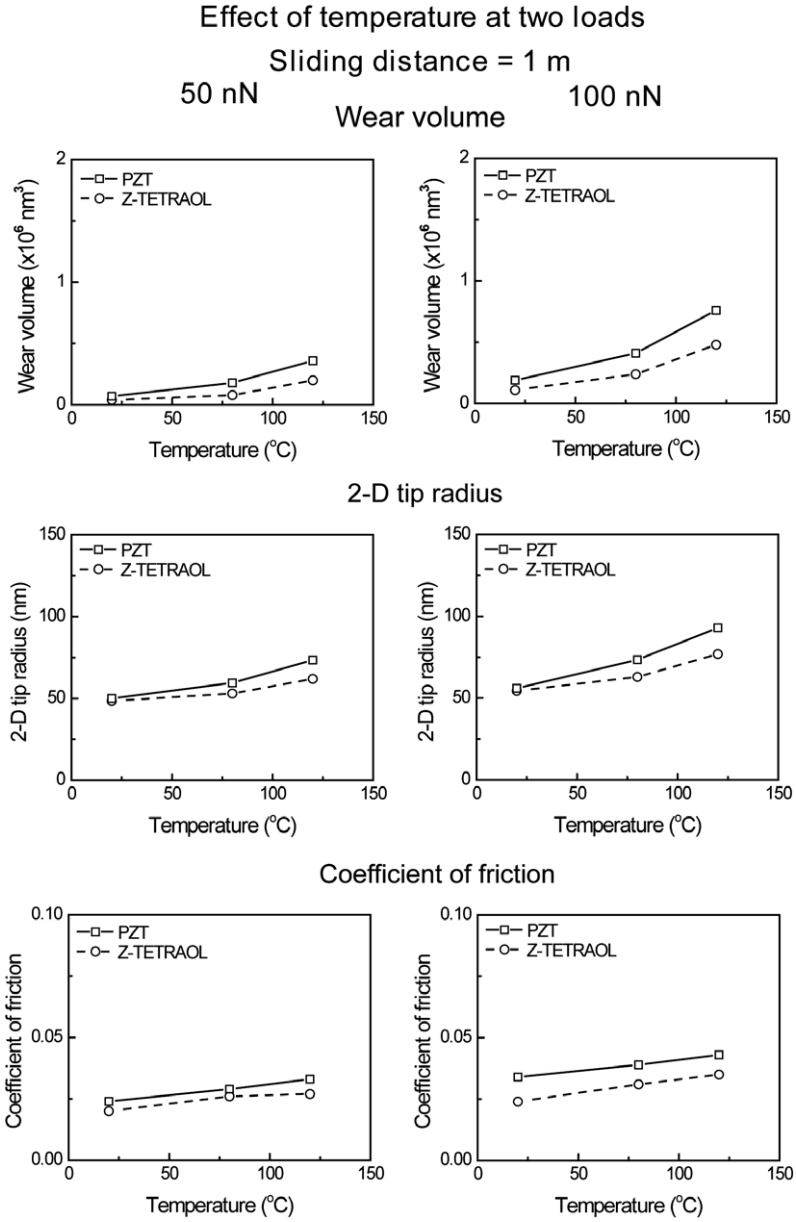

Figure 11. Wear volumes, 2D tip radii and coefficients of friction as a function of temperature at two loads on the unlubricated and Z-TETRAOL lubricated PZT films.

function of temperature at the ambient humidity. For the PZT film, domain walls and microstructure affect the mechanical and electrical properties (Setter *et al* 2006), which govern friction and wear behavior. The domain wall displacement is expected to occur with an increase of temperature, which is believed to be responsible for an increase in friction and wear. The relationship between the domain configuration and the microstructure and friction and wear properties still needs to be understood.

In the case of lubricant films, phase transformation occurs at high temperatures and is known to be responsible for changes in the friction (Yoshizawa *et al* 1993). In our experiments with PZT lubricated with a thin film of Z-TETRAOL, the effect of the temperature appears to be similar to that of the unlubricated PZT surface; thus, effect of temperature on the lubricated PZT is dominated by the PZT substrate. Lubricant merely reduces friction and wear at a given temperature.

3.4. Effect of relative humidity

Figure 12 shows the wear volume, tip radius and coefficient of friction data after 1 m sliding at 50 nN, after additional 1 m sliding at 100 nN and 0.1 mm s^{-1} at 5, 50 and 80% RH. Based on the data, the wear volume, tip radius and coefficient of friction increase with relative humidity. For the unlubricated PZT film, surface water layer is expected to develop, and its thickness should increase with relative humidity (figure 13). This increase in meniscus thickness is expected to result in an increase of meniscus force, and is responsible for an increase in

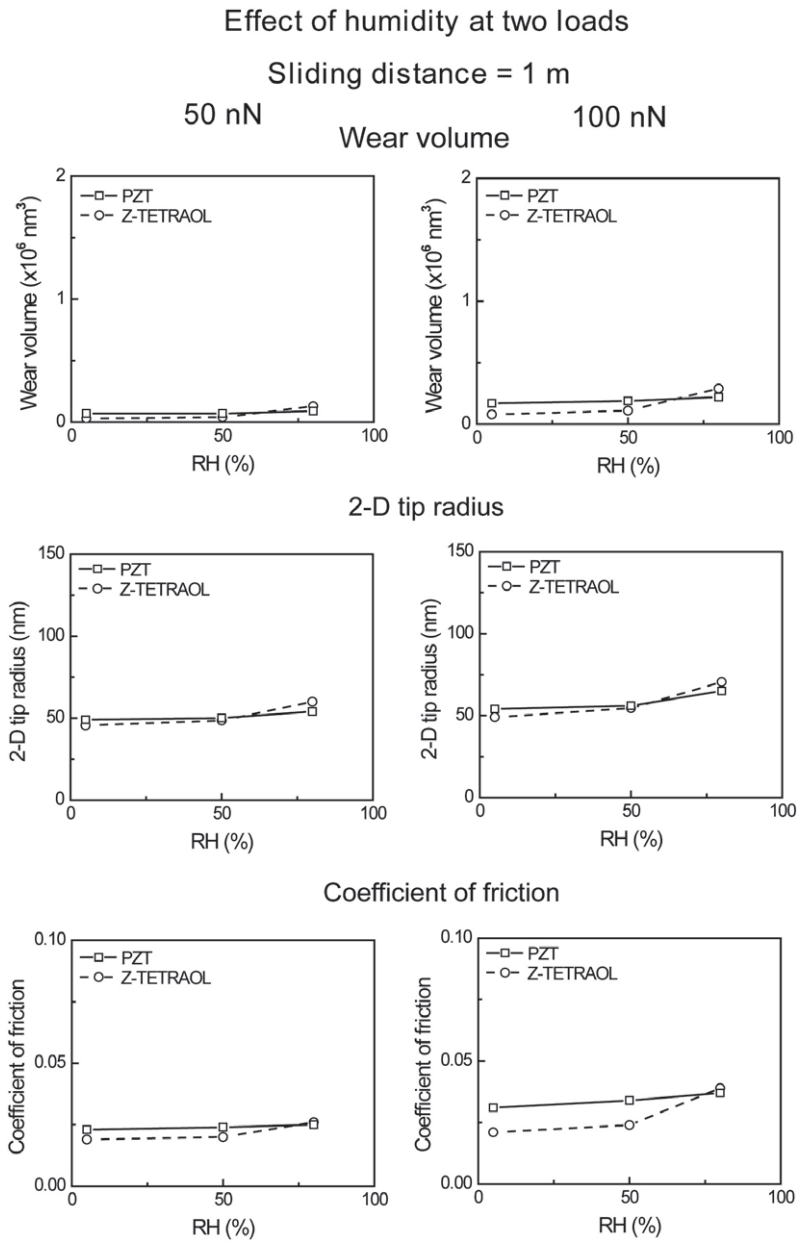

Figure 12. Wear volumes, 2D tip radii and coefficients of friction as a function of relative humidity at two loads on the unlubricated and Z-TETRAOL lubricated PZT films.

wear volume and friction (see solid lines in figure 12) (Bhushan 2002, 2005). The rate of increase of friction and wear is relatively constant during the entire humidity range.

In the case of the Z-TETRAOL lubricated film, the friction and wear increase slightly up to 50% RH and increase at a higher rate at higher humidity (see dotted lines in figure 12). Surface water molecules are expected to aggregate with mobile lubricant fractions of Z-TETRAOL and form a large meniscus, which is responsible for an increase in wear volume and coefficient of friction at a higher rate at high humidity of 80% RH (figure 13).

4. Conclusions

Two lubricants, Z-TETRAOL and BMIM-PF_6, were deposited on PZT films. Adhesion, friction and wear data for the Pt–Ir tips against the Z-TETRAOL lubricated PZT film are the lowest, followed by the BMIM-PF_6 lubricated PZT film. From AFM images, the wear scars of PZT against Pt–Ir tip show plowing of PZT material and pile up in the wear tracks, which is indicative of adhesive wear. From the SEM images of the worn tips, it is also deduced that the mechanism for tip wear is adhesive because the tip is plastically deformed. Tip profiles provide evidence of an irregular worn surface, indicating abrasive wear, especially after long sliding distances. Particles produced by the fracture of asperities stay between the contacting surfaces and could accelerate the abrasive wear.

Based on experiments on the effect of the velocity on tip wear, the sliding velocity appears to play a significant role. Wear and friction increase as a logarithm of velocity in lower

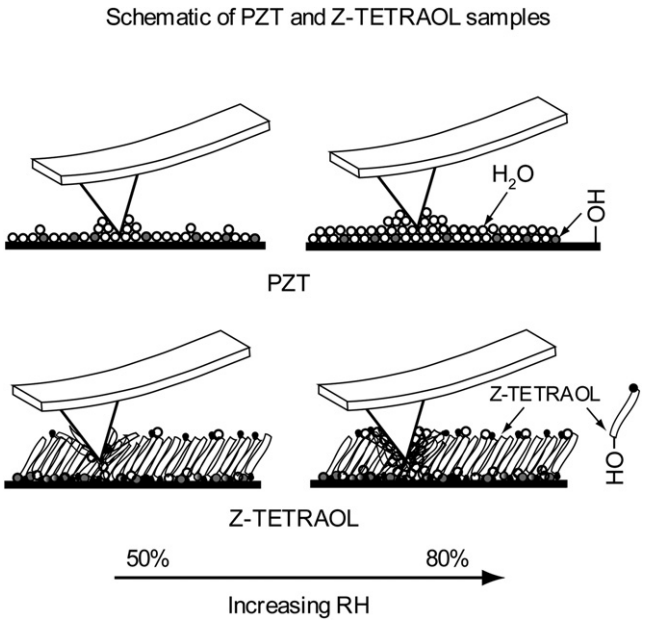

Figure 13. Schematic showing the change of meniscus between the AFM tip and the PZT samples, unlubricated and with Z-TETRAOL lubricated film, while increasing RH.

velocity range, which is based on the thermally-activated stick-slip mechanism. The wear increases slowly in higher velocity range, and is believed to be a combination of adhesive, abrasive and impact wear. From the high temperature experiments, wear and friction for both unlubricated and lubricated PZT increase with an increase in the sample temperature. The increase is believed to be associated with the degradation of the mechanical properties of PZT. The tip sliding on the Z-TETRAOL lubricated PZT exhibited lower wear volume and friction than those on unlubricated surfaces at a given temperature. Wear and friction increase with an increase in the relative humidity for both samples. At higher relative humidity, a thicker surface water layer is expected to develop which develops meniscus forces, responsible for an increase in wear volume and friction. For the Z-TETRAOL lubricated PZT, wear and friction increase with relative humidity with a larger rate of increase at relative humidity larger than 50% RH because of aggregation of water molecules with mobile lubricant.

This study advances the understanding of the physics of adhesion, friction and wear of Pt–Ir coated AFM probes.

References

Ahn C H, Tybell T, Antognazza L, Char Z, Hammond R H, Beasley M R, Fischer O and Triscone J M 1997 Local, nonvolatile writing of epitaxial $Pb(Zr_{0.52}Ti_{0.48})O_3/SrRuO_3$ heterostructures *Science* **276** 1100–3

Bhushan B 1996 *Tribology and Mechanics of Magnetic Storage Devices* 2nd edn (New York: Springer)

Bhushan B 2002 *Introduction to Tribology* (New York: Wiley)

Bhushan B 2005 *Nanotribology and Nanomechanics–An Introduction* 2nd edn (Heidelberg: Springer)

Bhushan B 2007 *Springer Handbook of Nanotechology* 2nd edn (Heidelberg: Springer)

Bhushan B and Kwak K J 2007a Platinum-coated probes sliding up to 100 mm s^{-1} against coated silicon wafers for AFM probe-based recording technology *Nanotechnology* **18** 345504

Bhushan B and Kwak K J 2007b Velocity dependence of nanoscale wear in atomic force microscopy *Appl. Phys. Lett.* **91** 163113

Bhushan B and Kwak K J 2008a Noble metal coated probes sliding at up to 100 mm/s against PZT films for AFM probe-based ferroelectric recording technology *J. Phys.: Condens. Matter* **20** 225013

Bhushan B and Kwak K J 2008b Effect of temperature on nanowear of platinum-coated probes sliding against coated silicon wafers for probe-based recording technology *Acta Mater.* **56** 380–6

Bhushan B, Palacio M and Kinzig B 2008 AFM-Based nanotribological and electrical characterization of ultrathin wear-resistant ionic liquid films *J. Colloid Interface Sci.* **317** 275–87

Campbell W E 1978 The lubrication of electrical contacts *IEEE Trans. Comp. Hybrids Manuf. Technol.* **1** 4–16

Davis J R 1998 *Metals Handbook: Desk Edition* 2nd edn (Materials Park, OH: ASM International)

Franke K, Besold J, Haessler W and Seegebarth C 1994 Modification and detection of domains on ferroelectric PZT films by scanning force microscopy *Surf. Sci.* **302** L283–8

Hidaka T, Maruyama T, Saitoh M, Mikoshiba N, Shimizu M, Shiosaki T, Willis L A, Hiskes R, Dicarolis S A and Amano J 1996 Formation and observation of 50 nm polarized domains in $PbZr_{1-x}Ti_xO_3$ thin film using scanning probe microscope *Appl. Phys. Lett.* **68** 2358–9

Kwak K J and Bhushan B 2008 Platinum-coated probes sliding at up to 100 mm/s against PZT films for atomic force microscopy probe-based ferroelectric recording technology *J. Vac. Sci. Technol.* A **26** 783–93

Liu H and Bhushan B 2003 Nanotribological characterization of molecularly thick lubricant films for applications to MEMS/NEMS by AFM *Ultramicroscopy* **97** 321–40

Palacio M and Bhushan B 2008a Nanotribological and nanomechanical properties of lubricated PZT thin films for ferroelectric data storage applications *J. Vac. Sci. Technol.* A **26** 768–76

Palacio M and Bhushan B 2008b Nanomechanical and nanotribological characterization of noble metal-coated AFM tips for probe-based ferroelectric data recording *Nanotechnology* **19** 105705

Palacio M and Bhushan B 2008c Ultrathin wear-resistant ionic liquid films for novel MEMS/NEMS applications *Adv. Mater.* **20** 1194–8

Ruan J and Bhushan B 1994 Atomic-scale friction measurements using friction force microscopy: part I—General principles and new measurement techniques *ASME J. Tribol.* **116** 378–88

Setter N, Damjanovic D, Eng L, Fox G, Gevorgian S, Hong S, Kingon A, Kohlstedt H, Park N Y, Stephenson G B, Stolichnov I, Taganstev A K, Taylor D V and Yamada T 2006 Ferroelectric thin films: review of materials, properties and applications *J. Appl. Phys.* **100** 051606

Shin H, Hong S, Moon J and Jeon J U 2002 Read/write mechanisms and data storage system using atomic force microscopy and MEMS technology *Ultramicroscopy* **91** 103–10

Tambe N S and Bhushan B 2005 Friction model for the velocity dependence of nanoscale friction *Nanotechnology* **16** 2309–24

Tao Z and Bhushan B 2005a Bonding, degradation and environmental effects on novel perfluoroether lubricants *Wear* **259** 1352–61

Tao Z and Bhushan B 2005b Degradation mechanisms and environmental effects on perfluoropolyether, self assembled monolayers, and diamondlike carbon films *Langmuir* **21** 2391–9

Tao Z and Bhushan B 2006a A new technique for studying nanoscale friction at sliding velocities up to 200 mm/s using atomic force microscope *Rev. Sci. Instrum.* **77** 103705

Tao Z and Bhushan B 2006b Surface modification of AFM silicon probes for adhesion and wear reduction *Tribol. Lett.* **21** 1–16

Tao Z and Bhushan B 2007 Velocity dependence and rest time effect on nanoscale friction of ultrathin films at high sliding velocities *J. Vac. Sci. Technol.* A **25** 1267–74

Van Valkenburg M E, Vaughn R L, Williams M and Wilkes J S 2002 Ionic liquids as thermal fluids *Electrochem. Soc. Proc.* **2002-19** 112–23

Villarrubia J S 1994 Morphological estimation of tip geometry for scanned probe microscopy *Surf. Sci.* **321** 287–300

Yoshizawa H, Chen Y L and Israelachvili J N 1993 Fundamental mechanisms of interfacial friction. 1. Relation between adhesion and friction *J. Phys. Chem.* **97** 4128–40